



Photocatalytic decolorization of methyl orange dye using nano- photocatalysts

Amin Ahmadpour^{1,*}, Mohsen Zare², Milad Behjoomanesh², Majid Avazpour²

¹Amirkabir Petrochemical Complex, Research and Technology Centre, Mahshahr, Iran

²Department of Chemical Engineering, Petroleum University of Technology, Ahwaz, Iran

ARTICLE INFO

Article history:

Received 23 February 2016

Received in revised form

17 June 2016

Accepted 18 June 2016

Keywords:

TiO₂/Fe₃O₄ and TiO₂/Fe₂O₃-nanocomposites

Ultrasonic-assisted deposition-precipitation method

Photocatalytic activity

Methyl orange

ABSTRACT

Environmental contamination, which is growing around the world, is a serious problem that cannot be neglected. Among all contaminations, water pollution is a major problem. Azo dyes are one of the largest groups of pollutants found in the drinking water, dyestuff and the food and textile industries. TiO₂/Fe₃O₄ and TiO₂/Fe₂O₃ nanocomposites with various ratios were synthesized by an ultrasonic-assisted deposition-precipitation method and their UV-light decolorization of methyl orange (MO) dye was investigated. The effect of Fe₃O₄/TiO₂ and Fe₂O₃-TiO₂ nanocomposites ratio on the photocatalytic activity and magnetic property of the nanocomposites was studied by comparing their decolorization curves and magnetism in the presence of magnet, respectively. The results revealed that the decolorization efficiency of 1 wt% Fe₃O₄/TiO₂ nanocomposite reached about 40% within 60 min UV irradiation at room temperature. However, this sample showed the least magnetism. Also, the ability of synthesized nanocomposites in holding the adsorbed methyl orange dye on their surface and the effect of pH were investigated.

1. Introduction

Many studies indicate that these dyes are toxic or carcinogenic [1]. During the last decades, because of hazardous problems that water pollution can cause for human [2-4], extensive attention has been paid to the study of more photocatalytic degradation of organic pollutants in water. The implementation of semiconductors, such as TiO₂ and ZnO as photocatalyst for purifying water has been the most interesting topic of recent studies [5, 6]. In such semiconductors, photogenerated carriers (electrons and holes) can tunnel to a reaction medium and participate in chemical reactions. Wider separation of the electrons and the holes enhances the efficiency of photocatalyst. Additionally, oxygen vacancy and defects strongly influence photocatalytic reactions [7]. In spite of the fact that many methods have been implemented to synthesize TiO₂ nanoparticles, after dispersing into waste water, it is difficult to re-collect them [8-10]. The problem of re-

collection has been solved by coating TiO₂ on the surface of magnetic core and using magnetic field to collect used photocatalyst. Whereas producing a core-shell of TiO₂/Fe₃O₄ requires a comprehensive dispersion of TiO₂ nanoparticles onto Fe₃O₄, synthesis of composite photocatalyst is 194 times more probable than core-shell photocatalyst. In this paper, the nanocomposite photocatalyst TiO₂/Fe₃O₄ with different ratios were synthesized by ultrasonic-assisted deposition-precipitation method. The magnetic property and photodecolorization of TiO₂/Fe₃O₄ nanocomposites were investigated. Furthermore, the efficiency and stability of the recycled nanocomposites were examined. In this paper, methyl orange (MO, C₁₄H₁₄N₃SO₃Na) was used as the pollutant. Methyl Orange is a common industrial dye favored for its stability and is categorized as an azo-dye. Azo-compounds, which are synthetic inorganic chemical compounds, account for up to 70% of the dyes in use nowadays. It is

*Corresponding author. Tel: +98-6522323630

E-mail address: ahmadpour_amin@yahoo.com

estimated that between 10-15% of the dye used in textile processing is lost and released as effluent. The release of this effluent is considered “non- aesthetic pollution” since amounts smaller than 1 ppm are visible in water sources. Although this is the primary motivation for degrading methyl orange, the dye waste water can also produce dangerous by-products during various chemical reactions such as oxidation and hydrolysis [11]. As noted, these azo-compounds are very stable, which is due to the large proportion of aromatics in the dye. Biological treatments may only de-color the dye effluents when opposed to degrading the effluent. A similar de-coloration phenomenon was discovered during this study for thermochemically ammonia treated Degussa P-25 TiO₂, and is discussed in detail below. Common physico-chemical treatments are effective in discoloration, but are also non-destructive. Instead, these treatments transfer the organic compounds from the water to another phase [11]. Due to the difficulty in degrading pollutants such as MO, a process referred to as Advanced Oxidation Process was proposed as an alternative to water purification. This process differs from the traditional oxidation by holes, with oxidation by a very reactive species such as hydroxyl radicals ($\bullet\text{OH}$). These reactive species can non-selectively oxidize a broad range of pollutants. It has been determined that heterogeneous photocatalysts, such as TiO₂, are the most destructive with regard to azo-compounds [12]. This destruction can be promoted by both artificial solar sources and sources employing solar technologies. The noted advantage to this method is that it is destructive, and can occur under ambient conditions. Further, it has been shown that it may lead to the complete mineralization of organic carbon into CO₂ [11].

2. Materials and methods

The samples were characterized by using scanning electron microscopy (SEM Holland Philips XL30 microscope). XRD patterns of the samples were recorded in ambient air using a Holland Xpert X-ray powder diffraction (XRD) (Cu K α , $\lambda=1.5406$). Average crystallite sizes of products were estimated using Scherrer's formula: $D= 0.9\lambda/(\beta \cos \theta)$ [11], where D is diameter of the nanoparticles, λ (Cu K α) =0.15406 nm and β is the full-width at half-maximum of the diffraction lines. The specific surface areas of the samples were also measured by Brunauer–Emmet–Teller (BET) method, using a Quanta chrome CHEMBET-3000 apparatus. The photoluminescence (PL) spectrum was recorded by applying a photoluminescence spectrophotometer (Avantes/Avaspec 2048) at room temperature in the

wavelength range of 200-1100 nm with the measurement accuracy of 0.04-20 nm. The band gaps of our samples were determined by UV-Visible spectrometer on an instrument PG T80 / T80+ with drift and solid cell. The spectra were recorded at room temperature in the wavelength range of 200-800 nm and accuracy of 0.5 nm. For purpose of assessment of the photocatalytic activity of the samples, a solution of 10 ppm (W/V) methyl orange (MO, C₁₄H₁₄N₃SO₃Na) was used. The photocatalytic experiments were carried out in beaker containing about 100 ml of methyl orange solution and about 50 mg of a photocatalyst sample. For providing desired UV photon, we implemented three UV-C (100-280 nm wavelength) lamps of 8 W (Philips, Holland) that were fixed at the height of 10 cm above the reaction vessel and irradiated perpendicularly to the surface of the solution. In order to saturate the solution with oxygen and also keep it homogenous, air pump that blows air into the solution and magnetic stirrer were used, respectively, during the irradiation. At the beginning of each experiment, we turned off the UV lamps for 15 minutes and then we turned them back on. Samples of the solution were obtained after 5, 15, 30, 60 min. The samples were centrifuged immediately to separate catalyst particles instantly. The methyl orange concentration of the solution was measured by a UV-visible spectrophotometer (UV-1600, Rayleigh). Absorption peak corresponding to methyl orange appeared at 462 nm. The concentration of dye in each decolorized sample was determined at max = 462 nm using a calibration curve. By means of this method, conversion percent of methyl orange azo dye can be obtained in different intervals. The degree of photodecolorization (X) is given by following formula:

$$X=(C_0 - C)/C_0 \quad (1)$$

Where, C₀ is the initial concentration of dye and C is the concentration of dye at different times [2].

3. Results and discussion

The XRD patterns of the TiO₂/Fe₃O₄ samples with different proportions of TiO₂ are presented in Fig. 1. Diffraction peaks of the TiO₂ anatase phase (JCPDS file No. 21-1272) and those of Fe₃O₄ (Fe₃O₄ in JCPDS file No. 19-0629) are indicated with the letters a and b in Fig. 1, respectively. As the molar ratio of TiO₂ to Fe₃O₄ increases, the diffraction peak intensities decrease, and as a subsequence yields a small contraction of lattice constants with the addition of Fe₃O₄. Moreover, no other characteristic peaks of the impurities are observed, which indicates the purity of the final products.

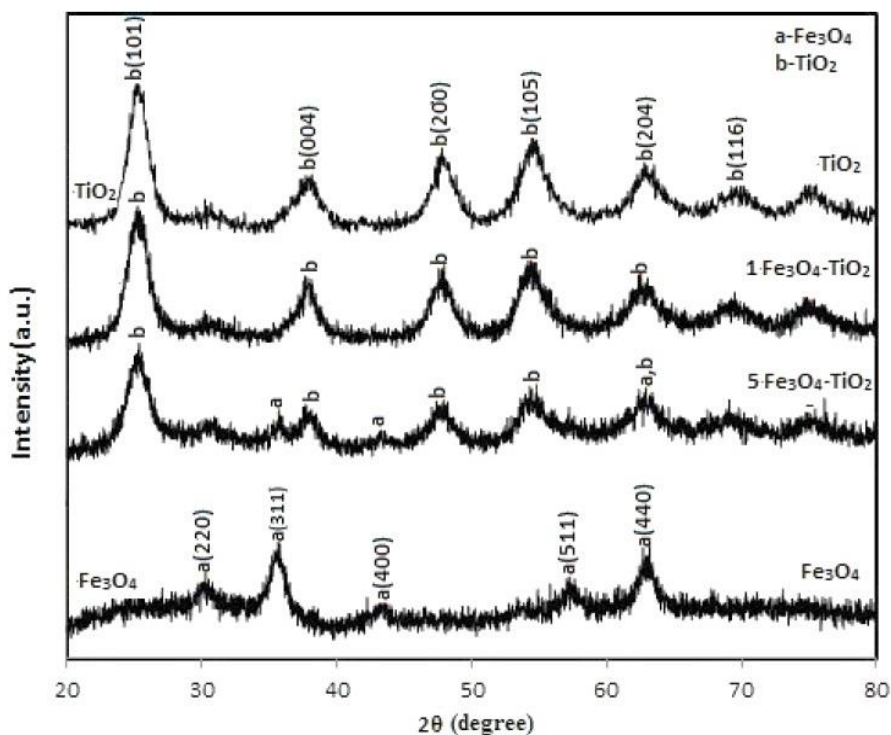


Fig. 1. The X-ray diffraction spectrum of TiO_2 , Fe_3O_4 , and $\text{TiO}_2/\text{Fe}_3\text{O}_4$ particles at various mole ratio of TiO_2 to Fe_3O_4 . The estimated crystallite sizes of the samples by the Scherrer's formula are shown in Table 1. The data shows that as the ratio of TiO_2 to Fe_3O_4 increases, the crystallite size decreases. FT1 sample has the smallest crystallite size of 3 nm.

Table 1. Crystallite size (calculated using the Scherrer formula), BET result, Band gap energy, samples of Decolorization percent.

Sample name	Materials	BET Surface area (m^2/g)	Crystallite Size (nm)	Band gap (eV)	% photo-Decolorization
F	Fe_3O_4	116	7	2.48	2
FT5	5.0 wt% $\text{Fe}_3\text{O}_4/\text{TiO}_2$	237	4	3.30	9
FT1	1.0 wt% $\text{Fe}_3\text{O}_4/\text{TiO}_2$	246	3	3.35	38
T	TiO_2	201	5	3.95	29

Specific surface areas of the samples determined by the BET method are also listed in Table 1. The surface area of the samples increases with an increase in the ratio of $\text{TiO}_2/\text{Fe}_3\text{O}_4$. FT1 shows the highest surface area of $246 \text{ m}^2/\text{g}$. This is in agreement with the crystallite size calculated from the broadening of XRD peaks. The morphologies of all samples were investigated by SEM. Fig. 2 (A-D) shows nearly spherical and uniform sizes of nanoparticles agglomeration of about 20-50 nm, the smallest and largest of which are for FT1 and F samples, respectively.

Figure 3 presents pictures of FT5 and FT1 powders in the solution with a magnet attached to the outside of the sample vials. The magnetic property of the samples declines when the content of TiO_2 increases and magnetism can be observed for FT1.

The absorption of UV-vis light is an important factor for the evolution of photocatalyst property. Also, it is useful to understand the structural variation of the materials via the calculated band gap values. The observed UV-vis absorption spectra of the samples are shown in Figure 4. It can be seen that a broad absorption band from ultraviolet to visible region and the maximum absorption peaks are found around 315.4, 370.5, 374.7, and 498.6 nm and their corresponding band gap values of 3.95, 3.35, 3.30, and 2.48 eV are observed for T, FT1, FT5, and F samples, respectively. Based on the maximum absorption wave, the band gaps of the samples are calculated [13].

$$E_g = 1240 \cdot \lambda^{-1} \quad (2)$$

where E_g is the band-gap energy (eV) and λ is the wavelength (nm).

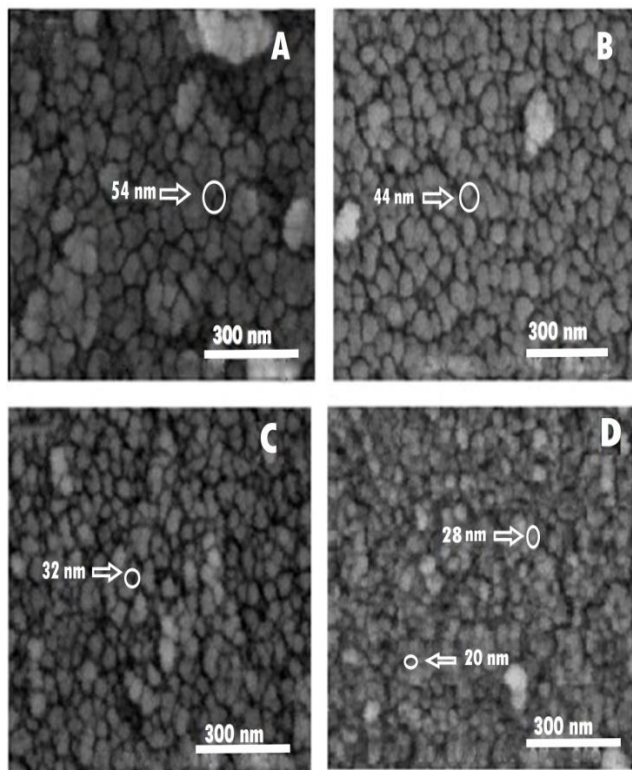


Fig. 2. SEM images of (A) Fe_3O_4 nanoparticles, (B) TiO_2 nanoparticles, (C) FT5 nanocomposites, (D) FT1 nanocomposites

In comparison with TiO_2 bulk ($E_g = 3.2$ eV), the band gap values of the prepared TiO_2 and $\text{TiO}_2/\text{Fe}_3\text{O}_4$ nanocomposites are shifted to higher energies with a blue shift. This blue shift suggests that band gaps have been found to be particle size dependent. The band gap of semiconductor nanocrystals increases with the decrease of its particle size, and the absorption edge will be blue-shifted due to the quantum effect. The band-gap of $\text{TiO}_2/\text{Fe}_3\text{O}_4$ photocatalysts (Table 1) is smaller than that of TiO_2 and increases with increasing the molar ratio of $\text{TiO}_2/\text{Fe}_3\text{O}_4$. The Fe^{3+} replaces Ti^{4+} dissociated from TiO_2 and then generates an interband trap that causes TiO_2 's absorption spectrum to red shift to the visible segment. FT1 shows a blue shift from the band gap of other nanocomposites, due to smaller crystallite sizes [14]. It is well known that optical absorption of photocatalysts significantly influences the activity of photocatalysts. Also, Photoluminescence (PL) signals and their intensity closely depend on its photocatalytic activity. PL spectra of the samples are shown in Fig. 5. Except Fe_3O_4 , all the samples exhibit two considerable broad PL signals at 465 and 530 nm. TiO_2 shows the highest intensity compared with the other samples. According to the literature [15, 16], the presence of these peaks in visible range is probably due to oxygen vacancies, defects, surface states, and other structural impurities.

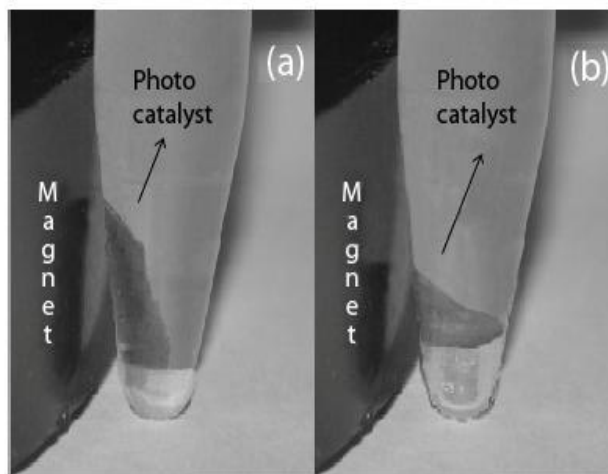


Fig. 3. Evaluation of magnetic properties. (a) FT5 and (b) FT1 nanocomposites.

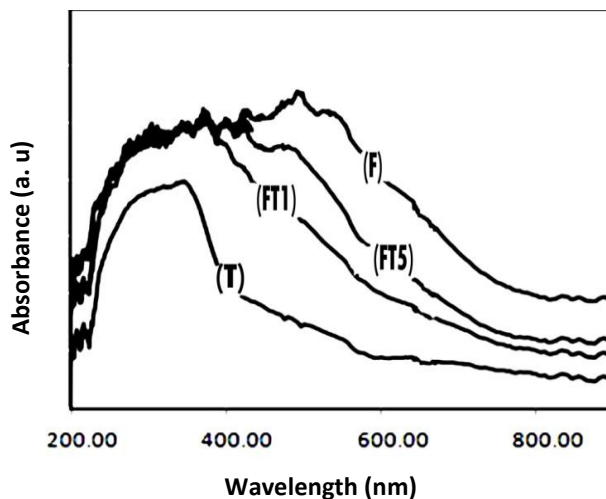


Fig. 4. The UV spectra of the samples (a) Fe_3O_4 nanoparticles (b) FT5 nanocomposites (c) FT1 nanocomposites

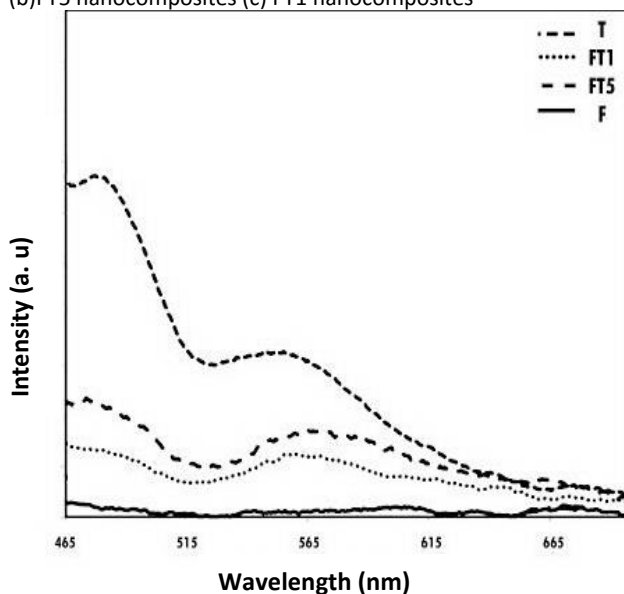


Fig. 5. The PL spectra of the samples

The prepared magnetic photocatalyst has a clear advantage over commercially available photocatalysts with its enhanced separation properties. However, in order to compete strongly, the magnetic photocatalyst also needs to have a comparable photoefficiency with these readily available photocatalysts. Thus the aim of the following work is to investigate the relationships between fundamental properties of the prepared photocatalyst particles and their photocatalytic activities, and also to develop a photocatalyst of high activity. The results of the photoactivity tests are given in Figure 6. The photocatalytic performance of the particles reaches for 15 minutes on stream (TOS) without irradiation (Dark) and for 60 min TOS under UV irradiation.

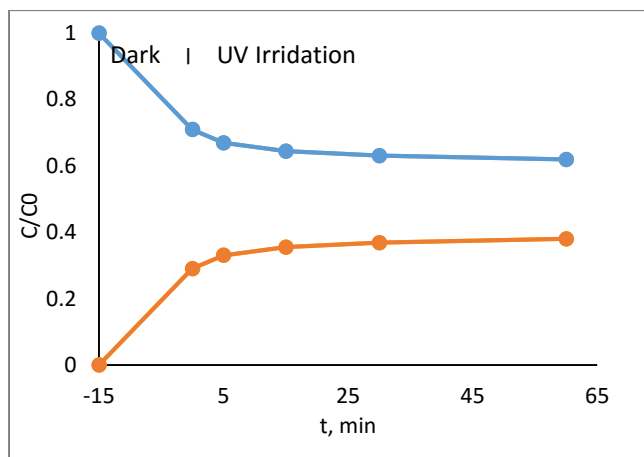


Fig. 6. The photocatalytic performance under UV irradiation and without irradiation

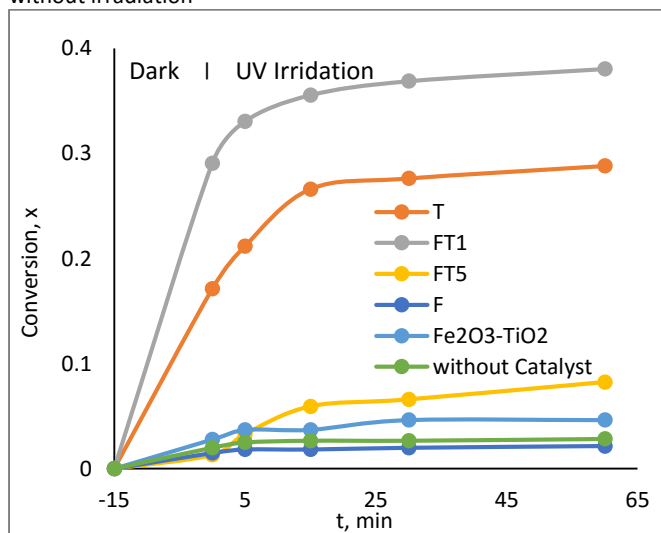


Fig. 7. The photocatalytic performance of different catalysts and ratios

When the photocatalysts were applied in the dark condition for about 15 min, the concentrations of methyl orange decreased and significant decolorization (29 %) is observed for FT1, which is probably due to the adsorption of more dye molecules on the surface of photocatalyst. This high adsorption may be attributed to its smallest crystalline size

and its highest surface area. The results show when the crystallite size decreases, the active sites increase. However, the magnetic property of this sample reduces due to decline in proportion of Fe_3O_4 to TiO_2 . Also, by substitution of Fe_3O_4 to Fe_2O_3 within nanocomposite TiO_2 , the decolorization of MO decreased significantly. In the presence of light, the result does not show desorption which verifies the high strength of the adsorption of methyl orange on the surface of samples. However, FT1 shows the highest photocatalytic efficiency of 38% in presence of UV light irradiation. It is well known that pH value has an influence on the rate of degradation of some organic compounds in photocatalytic processes [17]. The photodegradation of methyl orange was studied at five different pH values (2, 4, 6, 8, and 10) that is shown in Figure 8.

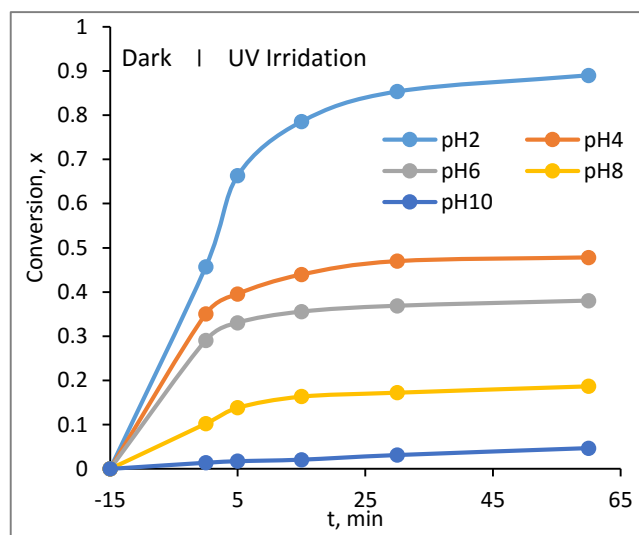


Fig. 8. The photodegradation of methyl orange at five different pH values

The pH was adjusted by the addition of 1 M HNO_3 at varied ratio for acidic pH of 2 and 4. For alkaline pH of 8 and 10, 0.1 M NaOH was used. The pH value is a complex parameter since it is related to the state of the photocatalyst surface, which affects the adsorption of MO on the photocatalyst [17]. From the Fig. 9, it was observed that the effect of pH on the degradation of the pollutants was variable. Several researches have been carried out to explain the effects of pH on photodegradation of dyes. The results indicated that the pH value of the pollutant was a key factor in dye degradation and changing the surface charge of the catalyst also influenced the photocatalytic reaction.

pH changed the adsorption of dye molecules onto the TiO_2 surface. For TiO_2 the pzc is around pH of 6.2. So, when pH value was less than 6 a strong adsorption of MO on the TiO_2 particles was observed as a result of electrostatic attraction of the positively charged TiO_2 with the dye. At alkaline pH, the MO molecules are negatively charged and their adsorption was also expected to change due to columbic repulsion. The effect of light wavelengths in UV and visible

range on MO decolorization using 0.05 g of FT1 photocatalyst was determined. Light intensity plays a major role in photodegradation. To study the effect of light intensity on the degradation of MO, the experiments were conducted at different light intensity. After dark reaction phenomenon was carried out, concentration of the MO solution was subjected to light intensity study. The intensity of the light has been varied by placing different lamps into the reactor. 1, 2, and 3 lamps were used and denoted as UV1, UV2 and UV3, respectively.

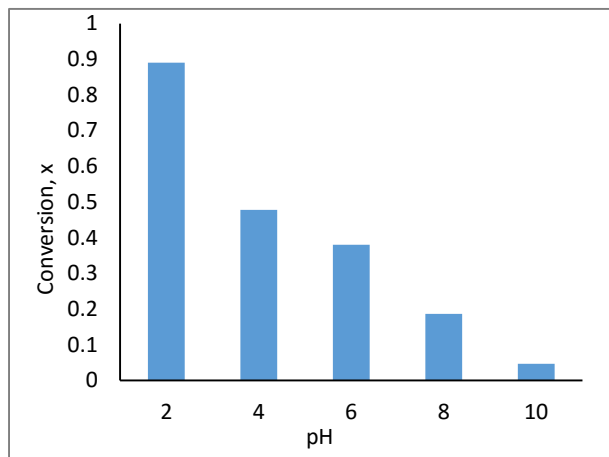


Fig. 9. The different effect of pH on the degradation of the pollutants.

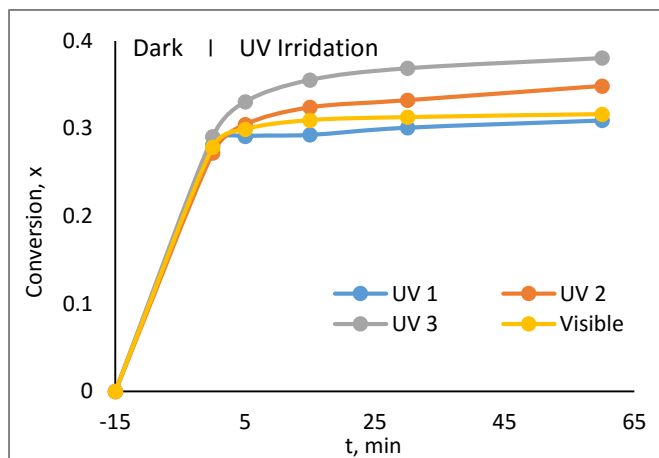


Fig. 10. The effect of light intensity and wavelength on the degradation.

From the Fig. 10 and Fig. 11, it can be explained that at lower intensities, the rate increases linearly as light intensity increases. While at higher intensities, the rate remained unaffected. This implies that at higher intensities the rate is independent of light intensity. This phenomenon occurred due to electron hole recombination competitiveness on catalyst composite surface with varying light intensity. Also, from Figure 10 it can be explained that, high intensity visible light has the same degradation in comparison to UV1.

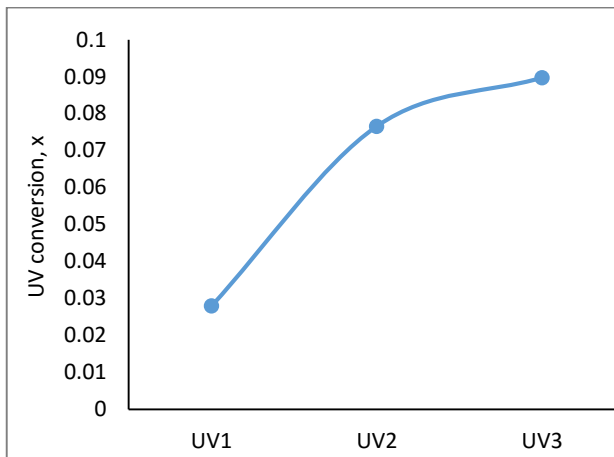


Fig. 11. The effect of light intensity



Fig. 12. The outer view of the reactor that decolorization operation happen inside it



Fig. 13. The inner space of the reactor that shows irradiation on the sample

4. Conclusions

TiO₂/Fe₃O₄ nanocomposites were synthesized by an ultrasonic-assisted deposition-precipitation method, and their photocatalytic decolorization of methyl orange and their ability to be separated by magnetite were investigated. As the TiO₂ content of the nanocomposite increases, the magnetic separability decreases and also when the TiO₂/Fe₃O₄ ratio increases, the crystallites sizes decrease and BET areas increase, leading to higher photocatalytic activity. The band gap of the nanocomposite decreases as the content of Fe₃O₄ increases. In the presence of light, the result does not show desorption which verifies the high strength of the adsorption of methyl orange on the surface of samples. However, FT1 shows the highest photocatalytic efficiency of 38% in presence of UV light irradiation. Also, by substitution of Fe₃O₄ to Fe₂O₃ within nanocomposite TiO₂, the decolorization of MO decreased significantly. The results indicated that the pH value of the pollutant was a key factor in dye degradation. At lower intensities the rate increases linearly as light intensity increases. While at higher intensities, the rate is independent of light intensity.

Acknowledgements

We would like to acknowledge Mr. A. Banisharif for providing the catalysts and his grateful guidance.

References

- [1] Richman, M. I. N. D. (1997). Industrial water pollution. *Wastewater*, 5(2), 24-29.
- [2] Firooz, A. A., Mahjoub, A. R., Khodadadi, A. A., Movahedi, M. (2010). High photocatalytic activity of Zn₂SnO₄ among various nanostructures of Zn_{2-x}Sn_{1-x}O₄ prepared by a hydrothermal method. *Chemical engineering journal*, 165(2), 735-739.
- [3] Parsaie, A., Haghiabi, A. H. (2015). Predicting the longitudinal dispersion coefficient by radial basis function neural network. *Modeling earth systems and environment*, 1(4), 1-8.
- [4] Parsaie, A., Haghiabi, A. H. (2015). Computational modeling of pollution transmission in rivers. *Applied water science*, 1-10.
- [5] Pare, B., Jonnalagadda, S. B., Tomar, H., Singh, P., Bhagwat, V. W. (2008). ZnO assisted photocatalytic degradation of acridine orange in aqueous solution using visible irradiation. *Desalination*, 232(1), 80-90.
- [6] Yassitepe, E., Yatmaz, H. C., Öztürk, C., Öztürk, K., Duran, C. (2008). Photocatalytic efficiency of ZnO plates in degradation of azo dye solutions. *Journal of photochemistry and photobiology A: Chemistry*, 198(1), 1-6.
- [7] Kong, J. Z., Li, A. D., Li, X. Y., Zhai, H. F., Zhang, W. Q., Gong, Y. P., Wu, D. (2010). Photo-degradation of methylene blue using Ta-doped ZnO nanoparticle. *Journal of solid state chemistry*, 183(6), 1359-1364.
- [8] Cozzoli, P. D., Kornowski, A., Weller, H. (2003). Low-temperature synthesis of soluble and processable organic-capped anatase TiO₂ nanorods. *Journal of the American chemical society*, 125(47), 14539-14548.
- [9] Jun, Y. W., Jung, Y. Y., Cheon, J. (2002). Architectural control of magnetic semiconductor nanocrystals. *Journal of the American chemical society*, 124(4), 615-619.
- [10] Rao, A. R., Dutta, V. (2007). Low-temperature synthesis of TiO₂ nanoparticles and preparation of TiO₂ thin films by spray deposition. *Solar energy materials and solar cells*, 91(12), 1075-1080.
- [11] Guettai, N., Amar, H. A. (2005). Photocatalytic oxidation of methyl orange in presence of titanium dioxide in aqueous suspension. Part I: Parametric study. *Desalination*, 185(1), 427-437.
- [12] Herrmann, J. M. (1999). Heterogeneous photocatalysis: fundamentals and applications to the removal of various types of aqueous pollutants. *Catalysis today*, 53(1), 115-129.
- [13] You, Y., Wan, L., Zhang, S., Xu, D. (2010). Effect of different doping methods on microstructure and photocatalytic activity of Ag₂O-TiO₂ nanofibers. *Materials research bulletin*, 45(12), 1850-1854.
- [14] Dong, X. L., Mou, X. Y., Ma, H. C., Zhang, X. X., Zhang, X. F., Sun, W. J., Xue, M. (2013). Preparation of CdS-TiO₂/Fe₃O₄ photocatalyst and its photocatalytic properties. *Journal of Sol-Gel science and technology*, 66(2), 231-237.
- [15] Luo, S., Fan, J., Liu, W., Zhang, M., Song, Z., Lin, C., Chu, P. K. (2006). Synthesis and low-temperature photoluminescence properties of SnO₂ nanowires and nanobelts. *Nanotechnology*, 17(6), 1695.
- [16] Liqiang, J., Xiaojun, S., Baifu, X., Baiqi, W., Weimin, C., Honggang, F. (2004). The preparation and characterization of La doped TiO₂ nanoparticles and their photocatalytic activity. *Journal of solid state chemistry*, 177(10), 3375-3382.
- [17] Prairie, M. R., Evans, L. R., Stange, B. M., Martinez, S. L. (1993). An investigation of titanium dioxide photocatalysis for the treatment of water contaminated with metals and organic chemicals. *Environmental science and technology*, 27(9), 1776-1782.